

# Analysis of the FWI workflow for accelerometer and DAS data from the 2018 CaMI VSP survey

Xiaohui Cai, Kris Innanen, Tianze Zhang, Kevin Hall, Matt Eaid

## ABSTRACT

In 2018, the Containment and Monitoring Institute Field Research Station (CaMI-FRS) in Newell County Alberta, which is part of CMC, carried out a 3D vertical seismic profile (VSP) (snowflake data) using three-component accelerometer and distributed acoustic sensing fibers (DAS). Eaid (2021a) have processed line 1 of the snowflake data to prepare them for inclusion in full waveform inversion. In this report, we mainly follow the processing and FWI workflow to inversion for the other line of the the snowflake data to detect the anisotropy of the area.

## INTRODUCTION

The Containment and Monitoring Institute Field Research Station (CaMI-FRS) under Carbon Management Canada (CMC) focuses on the development of technologies for monitoring injected CO<sub>2</sub> at its Field Research Station in Brooks, Alberta. To develop methods for monitoring the growth of a CO<sub>2</sub> plume maintained in Basal Belly River sandstone unit of Upper Cretaceous age at a depth of 300 meters (Isaac and Lawton, 2016), a vertical seismic profile (VSP) baseline survey, called snowflake, was acquired in 2018 using accelerometer and collocated distributed acoustic sensing fiber (DAS). Eaid (2021a and 2021b) have completed the processing and inversion for line 1 of the snowflake data last year. In this report, we perform inversion for the line 4 of the snowflake data to detect its anisotropy, where the accelerometer data, and DAS data are processed in order to prepare them for inclusion in full waveform inversion (Keating et al., 2021; Eaid et al., 2021a,b).

## FIELD DATA PROCESSING

Generally, the goal of processing field data for FWI is to only process the data to such an extent that it is a sufficiently close match to the modeled data. We extract the source line 4 (Figure 1) of snowflake data, where the injection well is also on line 4. The DAS and accelerometer data, will follow a similar overall processing workflow, but due to inherent differences in the two sensor types, each dataset will require slightly unique processing steps (Figure 2).

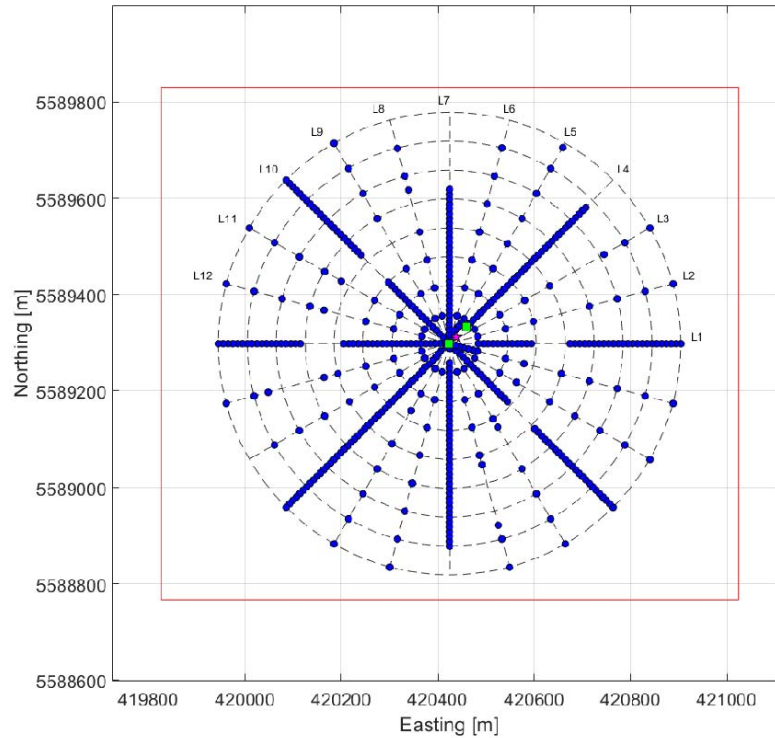


FIG. 1. Shot geometry of the CaMI-FRS 2018 3D walkaway-walkaround VSP. The blue circles represent shot point locations, the red squares the locations of the two observation wells (Observation well 2 is at the center of the shot points), and the green square the location of the injector well. The dotted lines are 60 meter concentric circles centered on observation well 2.

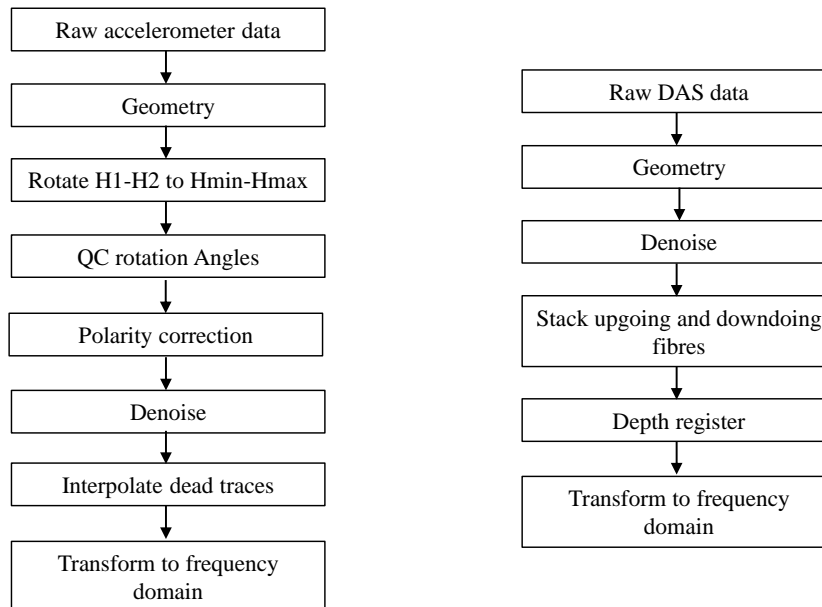


FIG. 2. Preprocessing workflow of the accelerometer data (left) and DAS data (right).

---

## Accelerometer data processing

### *Survey Geometry*

The first step in the processing workflow is to initialize the geometry for the survey. From the geometry (Figure 1), the line 4 shot points are located from northeast to southwest. The location of the observation well 2 is located at the center of the shot points, while the injection well is located at southwest of the observation well 2 with distance of 20 m. In reality, the well has a slight (maximum of  $9^\circ$ ) inclination from approximately 200 meters depth to the bottom of the well as measured on the accelerometer (Hall et al., 2018). However, the azimuth of the inclination is unknown, so this is unaccounted for in the geometry and subsequent modeling. The theoretical trace spacing for the designed acquisition is 1 m, however the cable for the accelerometer is not rigid and stretches over the length of the well resulting in increasing trace spacing with depth. Additionally, as previously stated the trace spacing shifts from 1 m to 2 m at a depth of 266.4 m due to the failure of the clamping mechanism of one of the strings. Source line 4 has a maximum offset of 390 m on southwest and 480 on northeast of observation well 2. Each shot is assigned a five digit shot point number, where the first two digits are the line number, and the last three digits are the shot number. The line 4 shot on the southwest edge is shot number 110. There are 82 shots and the shots almost increase for 10 meter shot spacing. Additionally, most of the signal occurs in the first 500 ms of the dataset, so the extracted line 4 dataset is windowed to the first 500 ms.

### *Processing*

- 1) Coordinate rotations and polarity correction. The accelerometer field data consist of the three orthogonal components of acceleration caused by the propagating wave-field, however, the horizontal components are orientated in an unknown and arbitrary direction that varies for each receiver. To ensure the horizontal data for each receiver samples a consistent azimuth, a coordinate rotation must be applied to each receiver so that the horizontal directions of each are aligned. In addition, The Hmax data are more coherent than the H1 and H2 datasets and consists of clear downgoing P-wave and S-wave energy, as well as reflections and mode conversions. The polarity of vertical component remains unchanged, and has an influence on the polarity of the horizontal component. Therefore, we use the QC Hodogram Display by Vista to rotate the H1 and H2 to the Hmax and Hmin dataset, and then adjust the polarity traces one by one. Figure 3 shows the accelerometer data after coordinate rotations and polarity correction for every 13th shot point on source line 4.
- 2) Noise attenuation. These accelerometer data have a relatively high signal-to-noise ratio, there are a few artifacts in the data that may present challenges for FWI. F-K denoising method is use in the process. Figure 4 shows the accelerometer data after denoising and low pass filtering for every 13th shot point on source line 4.
- 3) Trace interpolation. The dead traces are interpolated after a robust denoising algorithm. Figure 5 shows accelerometer data after trace interpolation for every 13th shot point on source line 4.

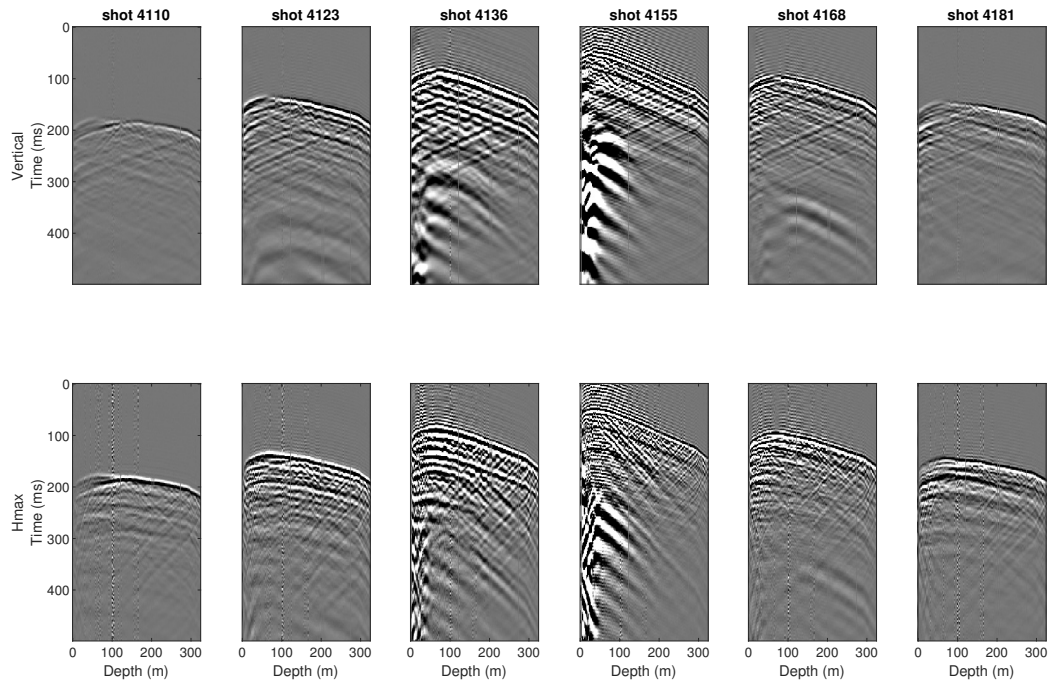


FIG. 3. Accelerometer data after coordinate rotations and polarity correction for every 13th shot point on source line 4. The top row plots the vertical component and the bottom row the Hmax component.

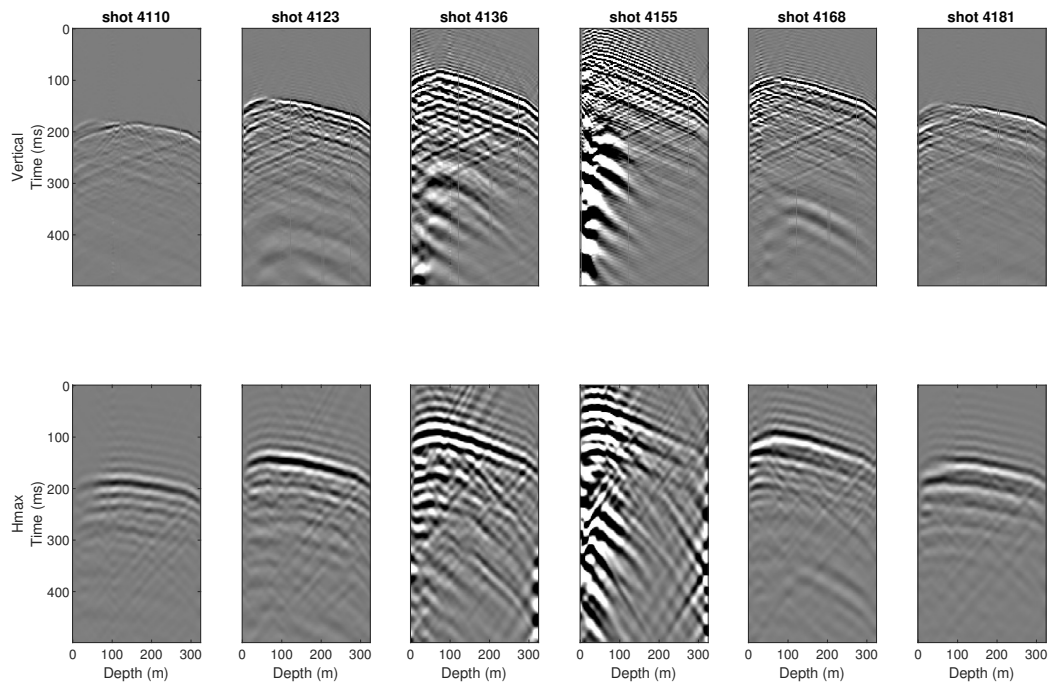


FIG. 4. Accelerometer data after denoising and low pass filtering for every 13th shot point on source line 4. The top row plots the vertical component and the bottom row the Hmax component.

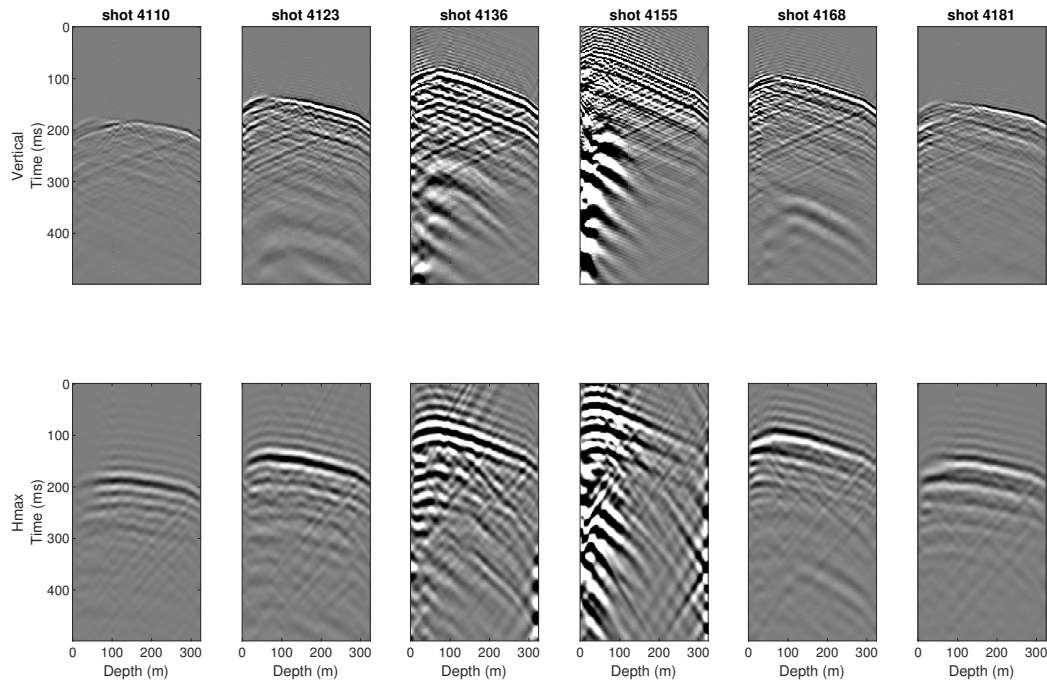


FIG. 5. Accelerometer data after trace interpolation for every 13th shot point on source line 4. The top row plots the vertical component and the bottom row the Hmax component.

## DAS data processing

### *Survey Geometry*

The processing flow use the minimally processing workflow to create data that supports full waveform inversion. The first step is to extract shot records on source line 4 over a window of 500 ms. Unfortunately, the interrogator unit failed to trigger for some of the shots, so the DAS dataset from source line 4 only has 74 shots, instead of the 82 shots on the accelerometer dataset.

### *Processing*

Figure 6 shows the raw straight DAS data for every 13th shot point on source line 4, while these data have a relatively high signal-to-noise ratio, there are a few artifacts in the data that may present challenges for FWI. F-K denoise method is use in the process (Figure 7). Then we stack the upging and downgoing fibres to get a better signal-to-noise ratio DAS data.

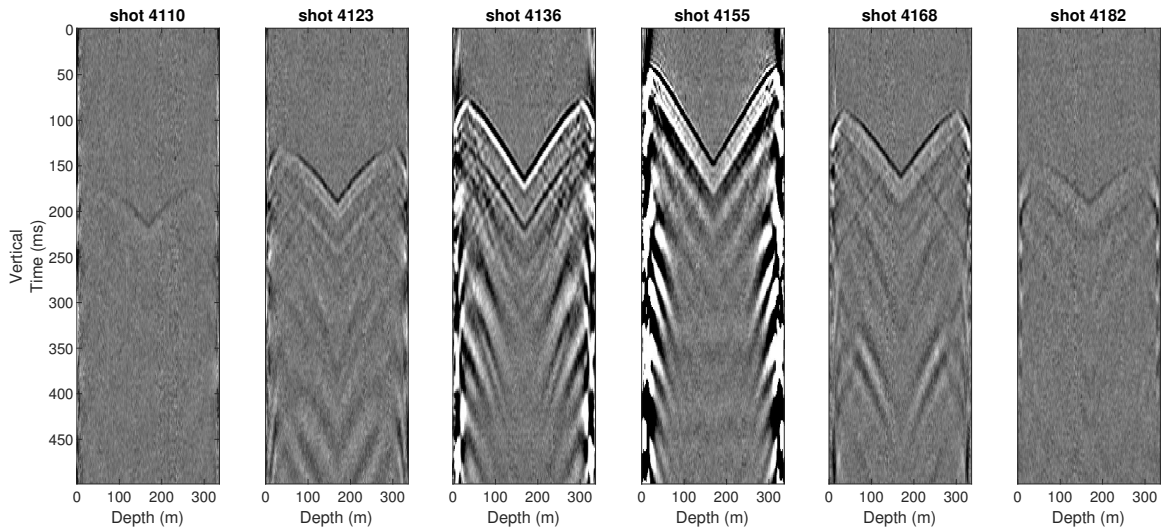


FIG. 6. Straight observation DAS data for every 13th shot point on source line 4.

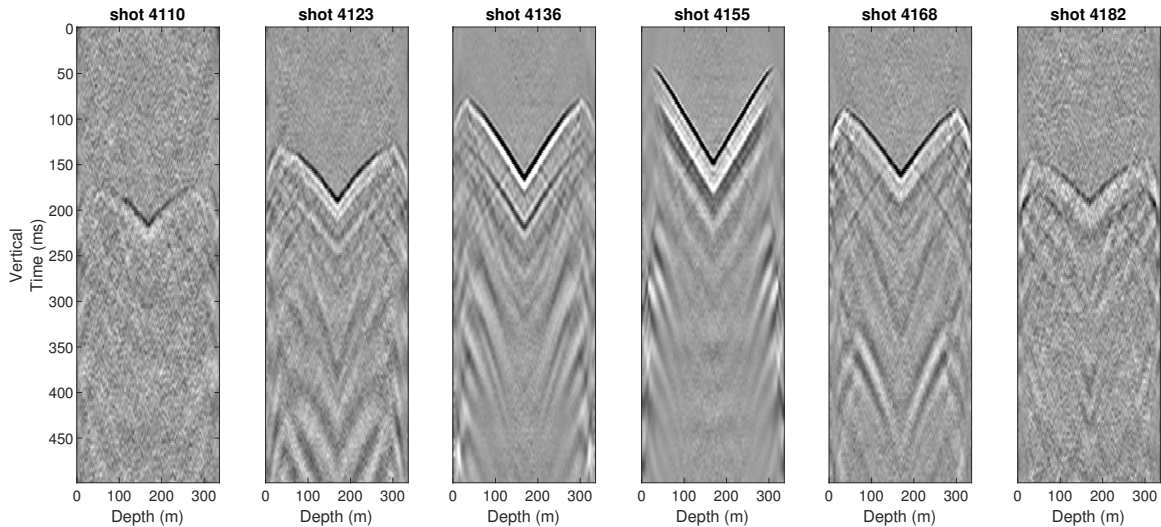


FIG. 7. Straight observation DAS data after denoising and low pass filtering for every 13th shot point on source line 4.

### *Depth registration*

Based on the phenomenon that das data has fixed intervals, we propose a depth registration method to obtain the depth of DAS data. According to the known depth of accelerometer data, we scan three parameters (starting depth, spatial interval, and the time difference between accelerometer data and DAS data). As shown in Figure 8, the depth in channel 2 is known (such as accelerometer data), we could calculate the depth of channel 1 using a start depth, a spatial interval and a time difference. Therefore, we can find the 7 traces in channel 2 closest to the 7 traces in channel 1, and then obtain the sum of the cross-correlation of the 7 traces of the two channels. Finally, we can get a maximum correlation coefficient and the corresponding time interval, starting depth and spatial interval, so as to get the depth of each trace of channel 1. Here, we get the depth of DAS data from 0 to 335.52 m with an

interval of 0.699 m. To demonstrate the accuracy of the DAS depth, we compared the first break time from shot 4170 for the accelerometer data and DAS data (Figure 9). It can be concluded that the depth obtained by our proposed method is suitable for these two types of the data. Figure 10 shows the DAS data after depth registered and stacking upping and downing fiber data for every 13th shot point on source line 4.

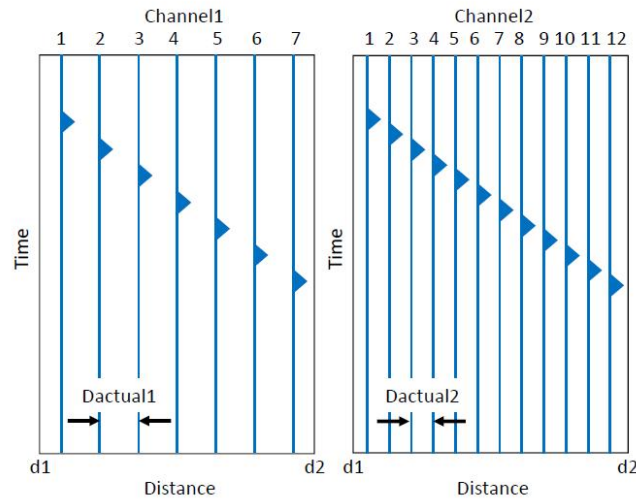


FIG. 8. Proposed method to estimate depth in Channel 1.

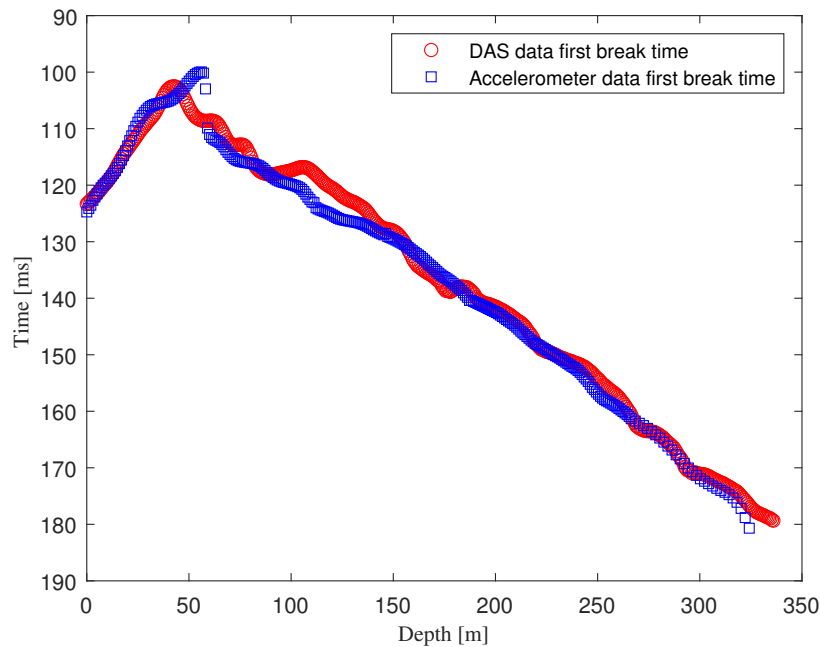


FIG. 9. First break picks from shot 4170 for the accelerometer data (blue) and DAS data (red).

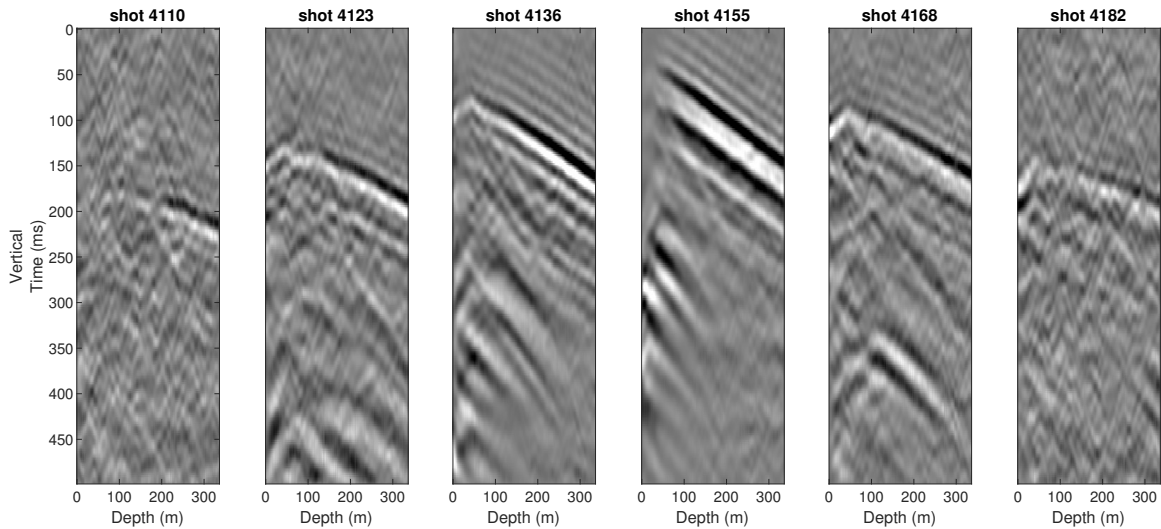


FIG. 10. DAS data after depth registered and stacking upping and downing fiber data for every 13th shot point on source line 4.

## FIELD DATA FWI

Here, we use P-wave velocity parameterization frequency-domain FWI and effective source estimation schemes to implement the elastic properties inversion (Cai et al., 2022). The model size is 840 m in the x-direction and 350 m in the z-direction, and the space interval is 5 m. In this report, we focus on frequencies between 10 Hz and 25 Hz. For the inversion, we consider five frequency bands, each consisting of seven frequencies, starting with the lowest frequencies and ending with a band spanning from low to high frequencies. The inversion approach could be divided into two steps: first is the source-only inversion and second is the simultaneous source and model inversion. For our implementation of the effective sources inversion strategy, we consider an effective source depth of 40 m. After source-only updates, we recalculate the amplitude scaling terms and proceed to model inversion. The inversion is performed over five frequency bands, with 10 iterations of L-BFGS optimization used at each band. The Figure 11 shows the inverted models of  $V_p$ ,  $V_s$ , and  $\rho$  for the line 4 and line 1 of the snowflake data, where the line 1 have been processed by Eaid last year (Eaid et al., 2021b). Figure 12 indicates the comparison of the initial and inverted velocities models with the well logs data. From the Figure 11 and Figure 12, we can see that the anisotropy exists in the field data.

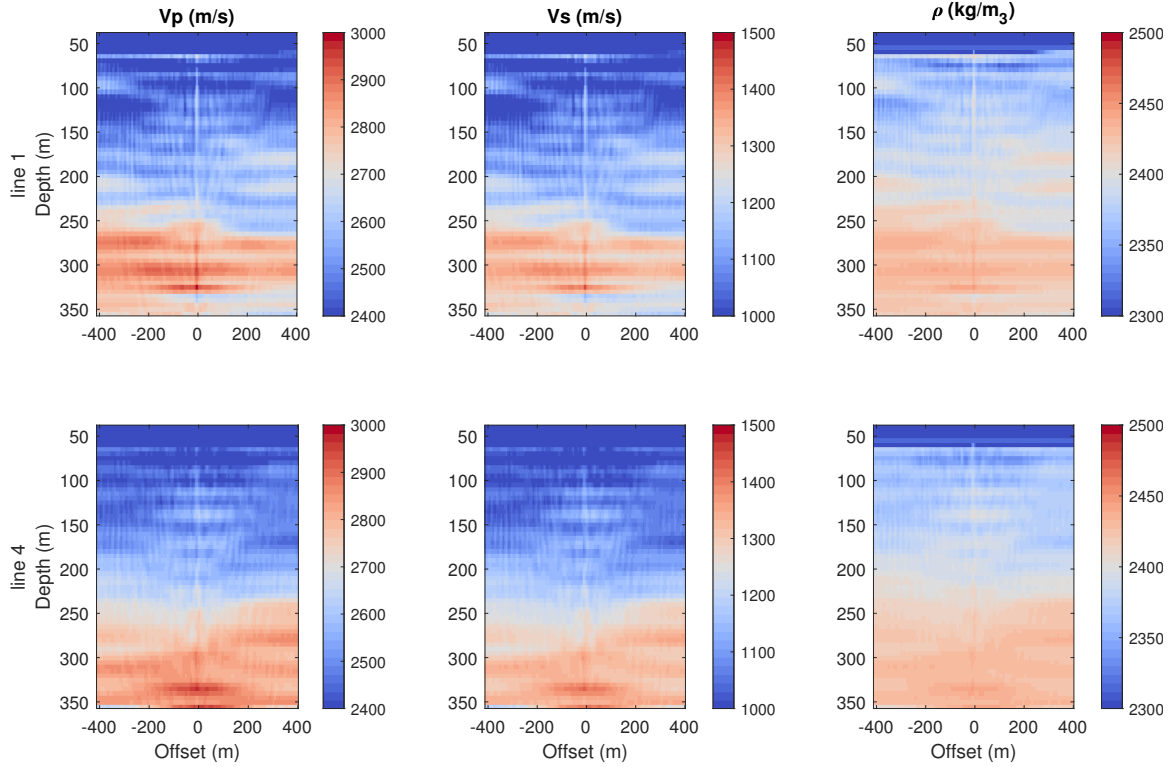


FIG. 11. Elastic FWI for the Line 1 and the Line 4 of the snowflake accelerometer and DAS data.

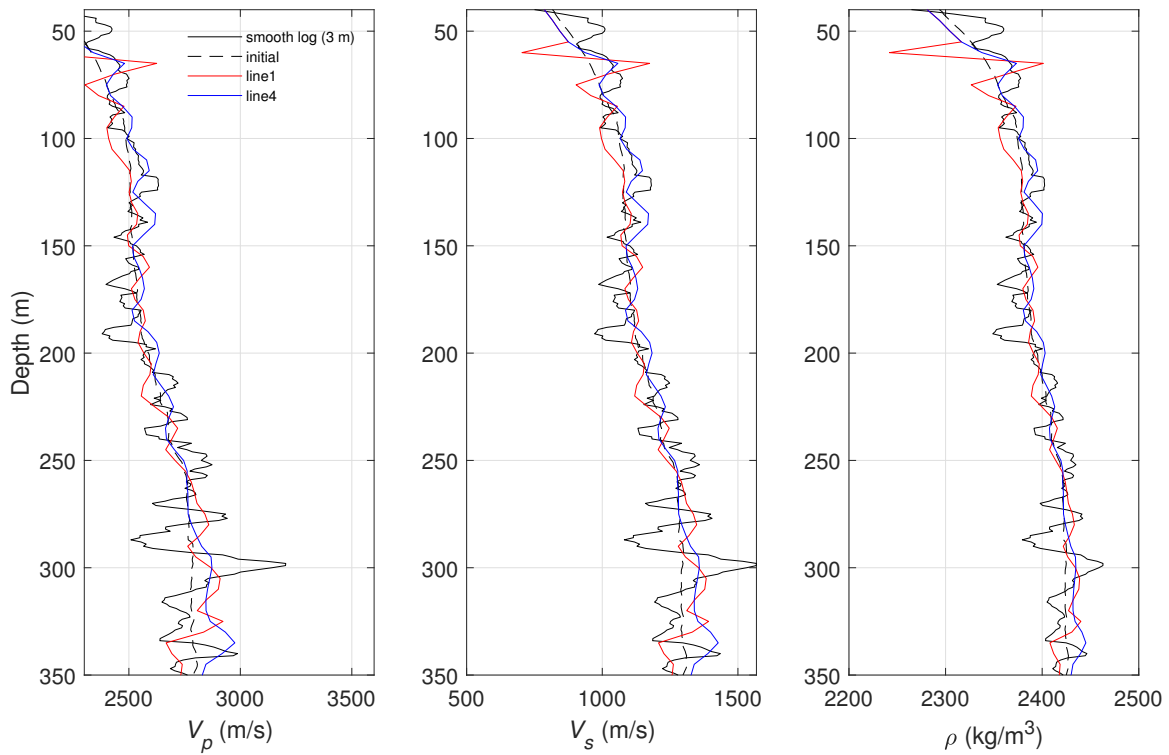


FIG. 12. The comparison of the initial and inverted velocities models (line 1 and line 4) with the well logs data.

## CONCLUSIONS

In this report, we perform full waveform inversion on a subset of the data collected in the 2018 CaMI VSP survey. we use log-derived  $V_p$  parameterization to help model convergence and explain the data as a full multiparameter inversion. In addition, the effective source approach are introduced to avoid many complications in near-surface land seismic data. The comparison of the inversion results of the line 1 and line 4 also indicate the anisotropy, but the anisotropy is not strong.

## ACKNOWLEDGMENTS

We thank the sponsors of CREWES for continued support. This work was funded by CREWES industrial sponsors and NSERC (Natural Science and Engineering Research Council of Canada) through the grant CRDPJ 543578-19. The data were acquired through a collaboration with the Containment and Monitoring Institute, Carbon Management Canada.

## REFERENCES

- Cai, X., Innanen, K., Hu, Q., Eaid, M., Keating, S., Hall, K., and Lawton, D., 2022, VSP imaging of CO<sub>2</sub> injection with rapid-repeat time lapse full waveform inversion: CREWES Research Reports.
- Eaid, M., Keating, S., and Innanen, K., 2021a, Full waveform inversion of DAS field data from the 2018 CaMI VSP survey: CREWES Report.
- Eaid, M., Keating, S., and Innanen, K., 2021b, Processing of the 2018 CaMI VSP survey for full waveform inversion: CREWES Report.
- Hall, K., Bertram, K., Bertram, M., Innanen, K., and Lawton, D., 2018, Crewes 2018 multi-azimuth walk-away VSP field experiment: CREWES Research Reports.
- Isaac, J. H., and Lawton, D. C., 2016, Brooks revisited: CREWES Research Reports.
- Keating, S., Eaid, M., and Innanen, K., 2021, Effective sources: removing the near surface from the VSP FWI problem: CREWES Report.